Heavy physics contributions to neutrinoless double beta decay from QCD

A. Nicholson,[1,2,*] E. Berkowitz,[3] H. Monge-Camacho,[4,5] D. Brantley,[4,6,5] N. Garron,[7] C.C. Chang,[5,8] E. Rinaldi,[9,5] M.A. Clark,[10] B. Joó,[11] T. Kurth,[12] B. Tiburzi,[13,14] P. Vranas,[6,5] and A. Walker-Loud[5,6,2]

[1]*Department of Physics and Astronomy, University of North Carolina, Chapel Hill, NC 27516-3255, USA*
[2]*Department of Physics, University of California, Berkeley, CA 94720, USA*
[3]*Institut für Kernphysik and Institute for Advanced Simulation, Forschungszentrum Jülich, 54245 Jülich Germany*
[4]*Department of Physics, The College of William & Mary, Williamsburg, VA 23187, USA*
[5]*Nuclear Science Division Lawrence Berkeley National Laboratory, Berkeley, CA 94720, USA*
[6]*Physics Division, Lawrence Livermore National Laboratory, Livermore, CA 94550, USA*
[7]*Theoretical Physics Division, Department of Mathematical Sciences, University of Liverpool, Liverpool L69 3BX, UK*
[8]*Interdisciplinary Theoretical and Mathematical Sciences Program (iTHEMS), RIKEN 2-1 Hirosawa, Wako, Saitama 351-0198, Japan*
[9]*RIKEN-BNL Research Center, Brookhaven National Laboratory, Upton, NY 11973, USA*
[10]*NVIDIA Corporation, 2701 San Tomas Expressway, Santa Clara, CA 95050, USA*
[11]*Scientific Computing Group, Thomas Jefferson National Accelerator Facility, Newport News, VA 23606, USA*
[12]*NERSC Lawrence Berkeley National Laboratory, Berkeley, CA 94720, USA*
[13]*Department of Physics, The City College of New York, New York, NY 10031, USA*
[14]*Graduate School and University Center, The City University of New York, New York, NY 10016, USA*

(Dated: May 11, 2018)

Observation of neutrinoless double beta decay, a lepton number violating process that has been proposed to clarify the nature of neutrino masses, has spawned an enormous world-wide experimental effort. Relating nuclear decay rates to high-energy, beyond the Standard Model (BSM) physics requires detailed knowledge of non-perturbative QCD effects. Using lattice QCD and taking advantage of effective field theory methods, we compute the model-independent leading-order matrix elements of short-range operators, which arise due to heavy BSM mediators, that contribute to this decay. Contributions from short-range operators may prove to be equally important to or even more important than those from long-range Majorana neutrino exchange.

Introduction.– Neutrinoless double beta decay ($0\nu\beta\beta$) is a process that, if observed, would reveal violations of symmetries fundamental to the Standard Model, and would guarantee that neutrinos have nonzero Majorana mass [1, 2]. Such decays can probe physics beyond the electroweak scale and expose a source of lepton-number (L) violation which may explain the observed matter-antimatter asymmetry in the universe [3, 4]. Existing and planned experiments will constrain this novel nuclear decay [5–16], but the interpretation of the resulting decay rates or limits as constraints on new physics will be a tremendous theoretical challenge.

The most widely discussed mechanism for $0\nu\beta\beta$ is that of a light Majorana neutrino, which can propagate a long distance within a nucleus. However, if the mechanism involves a heavy scale, $\Lambda_{\beta\beta}$, the resulting L-violating process can be short-ranged. While naïvely short-range operators are suppressed compared to long-range interactions due to the heavy mediator propagator, in the case of $0\nu\beta\beta$, the long-range interaction requires a helicity flip and is proportional to the mass of the light neutrino. In a standard seesaw scenario [17–21], this light neutrino mass is similarly suppressed by the same heavy mass scale, so the relative importance of long- versus short-range contributions is dependent upon the particle physics model under consideration and in general cannot be determined until the nuclear matrix elements involving both types of processes are computed.

Both long- and short-range mechanisms present substantial theoretical challenges if we hope to connect high energy physics with experimentally observed decay rates. The former case is difficult because one must understand long-distance nuclear correlations. In the latter case the short-distance physics is masked by QCD effects, requiring non-perturbative methods to match few-nucleon matrix elements to Standard Model operators.

Effective field theory (EFT) arguments show that at leading order (LO) in the Standard Model, there are nine local four-quark operators that can contribute to $0\nu\beta\beta$ decays [22, 23]. Further matching to a nuclear EFT [22] shows that, at leading order, there are up to three important processes—a negatively charged pion in the nucleus can be converted to a positively charged pion, releasing two electrons ($\pi\pi ee$ operators), a neutron can be converted to a proton plus a positively charged pion, also releasing two electrons ($NN\pi ee$ operators), and finally, two neutrons can be converted to two protons plus two electrons ($NNNNee$ operators). As long as the LO $\pi\pi ee$ are not forbidden by symmetries, the LO contribution to the nuclear $0\nu\beta\beta$ transition matrix element will be given by the $\pi\pi ee$ operators within the pion exchange diagram shown in the left panel of Figure 1.

In this Letter we determine the matrix elements of the relevant $\pi\pi ee$ operators and their associated low energy constants (LECs) for chiral perturbation theory (χPT) using lattice QCD (LQCD), a non-perturbative numeri-

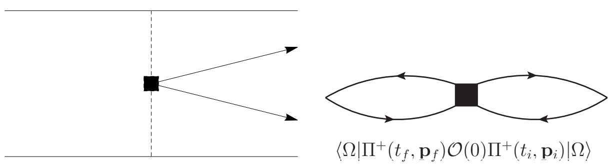

FIG. 1. Left: the leading order contribution to $0\nu\beta\beta$ via short-range operators occurs within a long-distance pion exchange diagram. The nucleons (solid lines) exchange charged pions (dashed), which emit two electrons (lines with arrowheads). Right: the LECs associated with the operators in the left panel may be calculated through a simpler $\pi^- \to \pi^+$ transition. Here, the lines represent quarks.

	$m_\pi \sim 310$ MeV		$m_\pi \sim 220$ MeV		$m_\pi \sim 130$ MeV	
a(fm)	V	$m_\pi L$	V	$m_\pi L$	V	$m_\pi L$
0.15	$16^3 \times 48$	3.78	$24^3 \times 48$	3.99		
0.12			$24^3 \times 64$	3.22		
0.12	$24^3 \times 64$	4.54	$32^3 \times 64$	4.29	$48^3 \times 64$	3.91
0.12			$40^3 \times 64$	5.36		
0.09	$32^3 \times 96$	4.50	$48^3 \times 96$	4.73		

TABLE I. List of HISQ ensembles used for this calculation, showing the volumes ($V = L^3 \times T$) studied for a given lattice spacing and pion mass.

cal method with fully controllable systematics. We perform extrapolations in all parameters characterizing deviations from the physical point, including quark mass and lattice spacing a, which controls effects from the discretization of space and time.

Method.– Using an EFT framework, it is not necessary to calculate the full $nn \to ppee$ transition shown in the left panel of Figure 1. Instead, we can perform the much more computationally tractable calculation of the on-shell $\pi^- \to \pi^+$ transition in the presence of external currents (four-quark operators). Once the LECs are determined, calculating the true off-shell process can be dealt with naturally within the EFT framework. From a LQCD perspective, this single pion calculation is computationally far simpler than the two nucleon calculation due to absence of a signal-to-noise problem [24] and complications in accounting for scattering states in a finite volume [25, 26].

We calculate matrix elements for the following relevant four-quark operators described in Ref. [22]:

$$\begin{aligned}
\mathcal{O}_{1+}^{++} &= \left(\bar{q}_L\tau^+\gamma^\mu q_L\right)\left[\bar{q}_R\tau^+\gamma_\mu q_R\right] \;, \\
\mathcal{O}_{2+}^{++} &= \left(\bar{q}_R\tau^+ q_L\right)\left[\bar{q}_R\tau^+ q_L\right] + \left(\bar{q}_L\tau^+ q_R\right)\left[\bar{q}_L\tau^+ q_R\right] \;, \\
\mathcal{O}_{3+}^{++} &= \left(\bar{q}_L\tau^+\gamma^\mu q_L\right)\left[\bar{q}_L\tau^+\gamma_\mu q_L\right] \\
&\quad + \left(\bar{q}_R\tau^+\gamma^\mu q_R\right)\left[\bar{q}_R\tau^+\gamma_\mu q_R\right] \;, \qquad (1)
\end{aligned}$$

where the Takahashi bracket notation () or [] indicates which color indices are contracted together [27]. We have omitted parity odd operators which do not contribute to the $\pi^- \to \pi^+$ transition, as well as the vector operators which are suppressed by the electron mass, as discussed in Ref. [22]. In addition, we calculate the color-mixed operators which arise through renormalization from the electroweak scale to the QCD scale [23]:

$$\begin{aligned}
\mathcal{O}_{1+}^{\prime\,++} &= \left(\bar{q}_L\tau^+\gamma^\mu q_L\right]\left[\bar{q}_R\tau^+\gamma_\mu q_R\right) \;, \\
\mathcal{O}_{2+}^{\prime\,++} &= \left(\bar{q}_L\tau^+ q_L\right]\left[\bar{q}_L\tau^+ q_L\right) + \left(\bar{q}_R\tau^+ q_R\right]\left[\bar{q}_R\tau^+ q_R\right) \qquad (2)
\end{aligned}$$

The analogous color-mixed operator $\mathcal{O}_{3+}^{\prime\,++}$ is identical to $\mathcal{O}_{3+}$ and is therefore omitted.

To determine the matrix elements for the $\pi\pi ee$ operators, we have performed a LQCD calculation using the publicly available highly-improved staggered quark (HISQ) gauge field configurations generated by the MILC collaboration [28, 29]. The set of configurations used is shown in Table I. With this set we perform extrapolations in the lattice spacing, pion mass, and volume. On these configurations we chose to produce Möbius domain wall quark propagators [30–32] due to their improved chiral symmetry properties, which suppresses mixing between operators of different chirality. To further improve the chiral properties, we first performed a gradient flow method to smooth the HISQ configurations [33–35], see Ref. [36] for details. This action has been successfully used to compute the nucleon axial coupling, g_A, with 1% precision [37–39]. For each ensemble we have generated quark propagators using both wall and point sources on approximately 1000 configurations.

The calculation of the matrix elements proceeds along the same lines as calculations of K^0- [40–48], D^0- [46, 49] and $B^0_{(s)}$-meson mixing [50–53] or $N\bar{N}$ oscillations [54, 55], and involves only a single light quark inversion from an unsmeared point source at the time where the four-quark operator insertion occurs. The propagators are then contracted to produce a pion at an earlier time (source) and later time (sink). Because no quark propagators connect the source to the sink, we can exactly project both source and sink onto definite momentum (allowing only zero momentum transfer at the operator) without the use of all-to-all propagators.

Results.– In Figure 2, we show representative plots on the near physical pion mass ensemble ($V = 48^3 \times 64$, $a = 0.12$ fm, $m_\pi \sim 130$ MeV), of the ratio

$$\mathcal{R}_i(t) \equiv C_i^{\rm 3pt}(t, T-t)/\left(C_\pi(t)C_\pi(T-t)\right) \;, \qquad (3)$$

where $C_i^{\rm 3pt}$ is the three-point function with a four-quark operator labeled by i at $t = 0$ and the sink (source) at time $t_f = t$ ($t_i = T - t$),

$$C_i^{\rm 3pt}(t_f, t_i) = \sum_{\mathbf{x},\mathbf{y},\alpha} \langle\alpha|\Pi^+(t_f,\mathbf{x})\mathcal{O}_i(0,\mathbf{0})\Pi^+(t_i,\mathbf{y})|\alpha\rangle \times e^{-E_\alpha T} \qquad (4)$$

where α labels QCD eigenstates, and the pion interpolating field is $\Pi^+ = (\Pi^-)^\dagger = \bar{d}\gamma_5 u$. C_π is the pion corre-

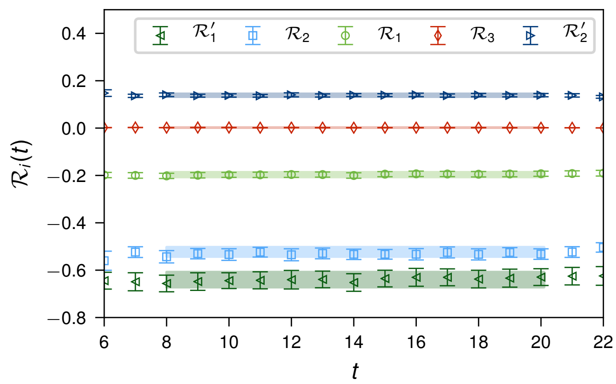

FIG. 2. An example of our lattice results for different operators on the near physical pion mass ensemble with $a \simeq 0.12$ fm.

lation function. Using relativistic normalization,

$$C_\pi(t) = \sum_{\mathbf{x}} \sum_\alpha \langle\alpha|\Pi^+(t,\mathbf{x})\Pi^-(0,\mathbf{0})|\alpha\rangle e^{-E_\alpha T}$$
$$= \sum_n \frac{|Z_n^\pi|^2}{2E_n^\pi}\left(e^{-E_n^\pi t} + e^{-E_n^\pi (T-t)}\right) + \cdots , \quad (5)$$

where $Z_n^\pi = \langle\Omega|\Pi^+|n\rangle$, Ω represents the QCD vacuum, and the $\cdots$ represent thermally suppressed terms. One can show that the ratio correlation function is given in lattice units by

$$\mathcal{R}_i(t) = \frac{a^4\langle\pi|\mathcal{O}_{i+}^{++}|\pi\rangle}{(a^2 Z_0^\pi)^2} + \mathcal{R}_{\text{e.s.}}(t)\,, \quad (6)$$

where $|\pi\rangle$ is the ground state pion and the excited state contributions are suppressed exponentially by their mass gap relative to the pion mass, $\mathcal{R}_{\text{e.s.}}(t) \propto e^{-(E_n^\pi - E_0^\pi)t}$. The overlap factors Z_π^0 are determined in the analysis of the two-point pion correlation functions. For brevity we henceforth write the matrix elements of these operators as $O_i = \langle\pi|\mathcal{O}_{i+}^{++}|\pi\rangle$ and attach a prime as appropriate.

We find excellent signals on nearly all ensembles, requiring only a simple fit to a constant. This is likely due to the fact that in the ratio defined in Equation 3 the contribution from the lowest thermal pion state is eliminated, which we find to be the leading contamination to the pion correlation function within the relevant time range. We also find little variation of the ratio using either wall or point sources. This gives us additional confidence that excited state contamination is negligible within the time range plotted in the left panel of Figure 2. A preliminary version of this analysis was presented in Ref. [56].

After extracting the matrix elements on each ensemble, we perform extrapolations to the continuum, physical pion mass, and infinite volume limits. It is straightforward to include these new operators in Chiral Perturbation Theory (χPT) [57] and to derive the virtual pion corrections which arise at next-to-leading order (NLO) in the chiral expansions,

$$O_1 = \frac{\beta_1\Lambda_\chi^4}{(4\pi)^2}\left[1 + \frac{7}{3}\epsilon_\pi^2 \ln(\epsilon_\pi^2) + c_1\epsilon_\pi^2\right],$$
$$O_2 = \frac{\beta_2\Lambda_\chi^4}{(4\pi)^2}\left[1 + \frac{7}{3}\epsilon_\pi^2 \ln(\epsilon_\pi^2) + c_2\epsilon_\pi^2\right],$$
$$\frac{O_3}{\epsilon_\pi^2} = \frac{\beta_3\Lambda_\chi^4}{(4\pi)^2}\left[1 + \frac{4}{3}\epsilon_\pi^2 \ln(\epsilon_\pi^2) + c_3\epsilon_\pi^2\right]. \quad (7)$$

In these expressions

$$\Lambda_\chi = 4\pi F_\pi\,, \qquad \epsilon_\pi = \frac{m_\pi}{\Lambda_\chi}\,, \quad (8)$$

where $F_\pi = F_\pi(m_\pi)$ is the pion decay constant at a given pion mass, normalized to be $F_\pi^{phys} = 92.2$ MeV at the physical pion mass, Λ_χ is the chiral symmetry breaking scale and ϵ_π^2 is the small expansion parameter for χPT. The pion matrix elements for $\mathcal{O}_{1+}^{\prime++}$ and $\mathcal{O}_{2+}^{\prime++}$ have an identical form to $\mathcal{O}_{1+}^{++}$ and $\mathcal{O}_{2+}^{++}$ respectively but have independent low-energy constants (LECs), β_i' and c_i' which describe the pion mass dependence. These expressions can be generalized to incorporate finite lattice spacing corrections [58] arising from the particular lattice action we have used [36] and finite volume corrections [59] which arise from virtual pions that are sensitive to the finite periodic volume used in the calculations. Details of the derivation of the formula in χPT and the extension to incorporate these lattice QCD systematic effects are presented in the supplemental material. In addition to the matrix elements O_i, the various LECs β_i and c_i are determined in this work.

The lattice QCD results are renormalized non-perturbatively following the Rome-Southampton method [60] with a non-exceptional kinematics symmetric point [61]. More precisely, we compute the relevant Z-matrix in the RI/SMOM (γ_μ, γ_μ)-scheme [62]. We implement momentum sources [63] to achieve a high statistical precision and non-perturbative scale evolution techniques [64, 65] to run the Z-factors to the common scale of $\mu = 3$ GeV. Further details about the renormalization procedure are provided in the supplemental material. One advantage of our mixed-action setup is that the renormalization pattern is the same as in the continuum (to a very good approximation) and does not require the spurious subtraction of operators of different chirality.

The renormalized operators, extrapolated to the continuum, infinite volume, and physical pion mass (defined by $m_\pi^{phys} = 139.57$ MeV and $F_\pi^{phys} = 92.2$ MeV) limits are given in Table II in both RI/SMOM and $\overline{\text{MS}}$ schemes at $\mu = 3$ GeV.

The correlation between these RI-SMOM matrix elements are given in the supplemental material. The extrapolations of these operators to the physical point are

TABLE II. Resulting matrix elements extrapolated to the physical point, renormalized in RI/SMOM and $\overline{\text{MS}}$, both at $\mu = 3$ GeV.

$O_i[\text{GeV}]^4$	RI/SMOM $\mu = 3$ GeV	$\overline{\text{MS}}$ $\mu = 3$ GeV
O_1	$-1.96(14) \times 10^{-2}$	$-1.94(14) \times 10^{-2}$
O_1'	$-7.21(53) \times 10^{-2}$	$-7.81(57) \times 10^{-2}$
O_2	$-3.60(30) \times 10^{-2}$	$-3.69(31) \times 10^{-2}$
O_2'	$1.05(09) \times 10^{-2}$	$1.12(10) \times 10^{-2}$
O_3	$1.89(09) \times 10^{-4}$	$1.90(09) \times 10^{-4}$

presented in Fig. 3 with the dashed vertical line representing the physical pion mass. The small value of O_3 reflects the fact that the $\mathcal{O}_{3+}^{++}$ operator is suppressed in the chiral expansion, vanishing in the chiral limit. In addition to the full MAEFT extrapolations (including infinite volume), we performed further extrapolations without including mixed-action and/or finite volume effects, and found all results to be consistent, indicating that mixed-action and finite volume effects are mild. These various analysis options are all available in Ref. [66] provided with this publication. Loss function minimization is performed using Ref. [67].

We can compare the values of the matrix elements determined here in $\overline{\text{MS}}$ to those in Ref. [68], which used $SU(3)$ flavor symmetry to determine the values, including estimated $SU(3)$ flavor-breaking corrections at NLO in $SU(3)$ χPT. Noting the differences in operator definition pointed out in footnote 5 of Ref. [68], we find the values of the matrix elements tend to agree at the one- to two-sigma level, as measured by the O$(20-40\%)$ uncertainties in Ref. [68], indicating the $SU(3)$ chiral expansion is reasonably well behaved. With $N_{sample} \sim 1000$ in the LQCD calculations presented here, the uncertainties have been reduced to O$(5-8\%)$. The resulting LECs are reported in Tab. III in the supplemental material and the full covariance between them is provided in Ref. [66].

From the matrix element O_3 we can determine the value of B_π, the bag parameter of neutral meson mixing in the Standard Model, $B_\pi = O_3/(\frac{8}{3}m_\pi^2 F_\pi^2) = 0.430(16)\,[0.432(16)]$ in the RI/SMOM [$\overline{\text{MS}}$] scheme at $\mu = 3$ GeV. This is a rather low value, indicating a large deviation from the vacuum saturation approximation. However this is expected from the chiral behavior as discussed, for example, in Ref. [69–71]. As displayed in Fig. 4 in the supplemental material, the value of B_π increases at larger pion masses, as expected.

Discussion. – We have performed the first LQCD calculation of hadronic matrix elements for short-range operators contributing to $0\nu\beta\beta$. This calculation is complete for matrix elements contributing to leading order in χPT, including extrapolation to the physical point in both lattice spacing and pion mass. We have also performed calculations directly at the physical pion mass.

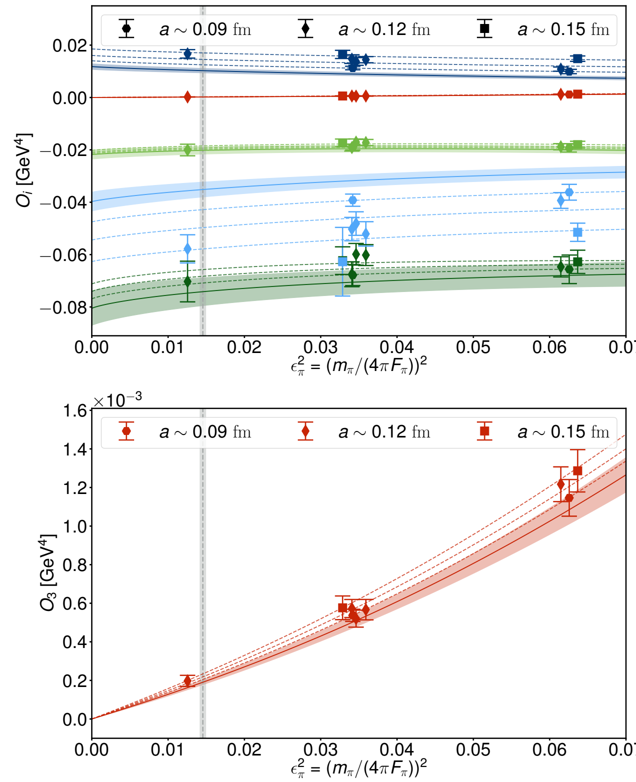

FIG. 3. The interpolation of the various matrix elements (color coded as in Fig. 2). In the bottom panel, a zoomed in version of O_3 is displayed. The resulting fit curves/bands are constructed with Λ_χ held fixed while changing ϵ_π and so the corresponding LQCD results are adjusted by $(F_\pi^{phys}/F_\pi^{latt})^4$ for each lattice ensemble to be consistent with this interpolation. The bands represent the 68% confidence interval of the continuum, infinite volume extrapolated value of the matrix elements. The vertical gray band highlights the physical pion mass.

Given these $\pi^- \to \pi^+$ matrix elements, the nuclear beta decay rate can be determined by constructing the $nn \to pp$ potential that they induce. The strong contribution to this potential for matrix element O_i is given by

$$V_i^{nn\to pp}(|\mathbf{q}|) = -O_i P_{1+} P_{2+} \frac{\partial}{\partial m_\pi^2} V_{1,2}^{\pi}(|\mathbf{q}|)$$
$$= -O_i \frac{g_A^2}{4F_\pi^2} \tau_1^+ \tau_2^+ \frac{\sigma_1 \cdot \mathbf{q}\, \sigma_2 \cdot \mathbf{q}}{(|\mathbf{q}|^2 + m_\pi^2)^2}\,, \qquad (9)$$

where $V_{1,2}^{\pi}(|\mathbf{q}|) = -\tau_1 \cdot \tau_2\, \sigma_1 \cdot \mathbf{q}\, \sigma_2 \cdot \mathbf{q}/(|\mathbf{q}|^2 + m_\pi^2)$ is the long-range pion-exchange potential between two nucleons (labeled 1 and 2) and $P_{1,2}^+$ project onto the isospin raising operator for each nucleon. This potential needs to be multiplied by the electrons $\bar{e}e^c$, the overall prefactor $\frac{G_F^2}{\Lambda_{\beta\beta}}$ and the Wilson coefficient of the effective Standard Model operators for a given heavy physics model to determine the full $nn \to ppe^- e^-$ amplitude. These matrix elements, once incorporated into nuclear decay rate calculations, can be used to place limits on the various BSM mechanisms that give rise to $0\nu\beta\beta$, see for example [22, 23, 72–81]. The limits on the BSM mechanisms must also account for the running of these short distance operators, which can modify their strength by an amount comparable to the current uncertainties on the nuclear matrix elements themselves [82].

Modern analyses use Effective Field Theory [22, 23, 80, 81], for which this contribution is the leading order short-range correction. To go beyond leading order in χPT additional calculations are necessary. For planned experiments probing $0^+ \to 0^+$ nuclear transitions, all next-to leading order diagrams of type $NN\pi ee$ vanish due to parity [22]. At next-to-next-to leading order there exist both $NN\pi ee$ diagrams and $NNNNee$ contact diagrams. Calculation of the $NNNNee$ contact contribution may prove important, as diagrams involving light pion exchange may need to be summed non-perturbatively in the EFT framework, causing the contact to be promoted to LO (as was found for the light neutrino exchange diagrams in Ref. [83]). While computing the $NNNNee$ contact interaction will prove challenging, it is in principle calculable with current technology and resources [84]. Finally, in order to disentangle long- and short-range $0\nu\beta\beta$ effects, investigation of quenching of the axial coupling, g_A, in multi-nucleon systems [85–87], as well as the isotensor axial polarizability [88, 89], will also be useful.

Our results can in principle be used to determine contributions from any BSM model leading to short-range $0\nu\beta\beta$ to leading order in χPT. However, these results must first be incorporated into nuclear physics models capable of describing large nuclei. Currently, there is sizable discrepancy between different models and uncertainty quantification remains difficult, challenges which will need to be overcome in order to faithfully connect experiment with theory.

Acknowledgments: We thank Emanuele Mereghetti and Vincenzo Cirigliano for helpful conversations and correspondence. Numerical calculations were performed with the `Chroma` software suite [90] with `QUDA` inverters [91, 92] on Surface at LLNL, supported by the LLNL Multiprogrammatic and Institutional Computing program through a Tier 1 Grand Challenge award, and on Titan, a resource of the Oak Ridge Leadership Computing Facility at the Oak Ridge National Laboratory, which is supported by the Office of Science of the U.S. Department of Energy under Contract No. DE-AC05-00OR22725, through a 2016 INCITE award. The calculations were efficiently interleaved with those in Ref. [37–39] using `METAQ` [93].

This work was supported by the NVIDIA Corporation (MAC), the DFG and the NSFC through funds provided to the Sino-German CRC 110 "Symmetries and the Emergence of Structure in QCD" (EB), a RIKEN SPDR fellowship (ER), the Leverhulme Trust (NG), the U.S. Department of Energy, Office of Science: Office of Nuclear Physics (EB, DAB, CCC, TK, HMC, AN, ER, BJ, PV, AWL); Office of Advanced Scientific Computing (EB, BJ, TK, AWL); Nuclear Physics Double Beta Decay Topical Collaboration (DAB, HMC, AWL, AN); and the DOE Early Career Award Program (DAB, CCC, HMC, AWL) and the LLNL Livermore Graduate Scholar Program (DAB). This work was performed under the auspices of the U.S. Department of Energy by LLNL under Contract No. DE-AC52-07NA27344 (EB, ER, PV), and by LBNL under Contract No. DE-AC02-05CH11231, under which the Regents of the University of California manage and operate LBNL. This research was supported in part by the National Science Foundation under Grant No. NSF PHY-1748958, and parts of this work were completed at the program "Frontiers in Nuclear Physics" (NUCLEAR16).

* annichol@email.unc.edu

[1] Joseph Schechter and José WF Valle, "Neutrinoless double-β decay in $su(2) \times u(1)$ theories," Physical Review D **25**, 2951 (1982).

[2] Martin Hirsch, Sergey Kovalenko, and Ivan Schmidt, "Extended black box theorem for lepton number and flavor violating processes," Phys. Lett. **B642**, 106–110 (2006), arXiv:hep-ph/0608207 [hep-ph].

[3] S. Pascoli, S. T. Petcov, and Antonio Riotto, "Leptogenesis and Low Energy CP Violation in Neutrino Physics," Nucl. Phys. **B774**, 1–52 (2007), arXiv:hep-ph/0611338 [hep-ph].

[4] Sacha Davidson, Enrico Nardi, and Yosef Nir, "Leptogenesis," Phys. Rept. **466**, 105–177 (2008), arXiv:0802.2962 [hep-ph].

[5] M. Agostini *et al.*, "Background-free search for neutrinoless double-β decay of ^{76}Ge with GERDA," (2017), 10.1038/nature21717, [Nature544,47(2017)], arXiv:1703.00570 [nucl-ex].

[6] S. Andringa *et al.* (SNO+), "Current Status and Future Prospects of the SNO+ Experiment," Adv. High Energy Phys. **2016**, 6194250 (2016), arXiv:1508.05759 [physics.ins-det].

[7] S. R. Elliott *et al.*, "Initial Results from the MAJORANA DEMONSTRATOR," *Proceedings, 27th International Conference on Neutrino Physics and Astrophysics (Neutrino 2016): London, United Kingdom, July 4-9, 2016*, J. Phys. Conf. Ser. **888**, 012035 (2017), arXiv:1610.01210 [nucl-ex].

[8] A. Gando *et al.* (KamLAND-Zen), "Limit on Neutrinoless $\beta\beta$ Decay of ^{136}Xe from the First Phase of KamLAND-Zen and Comparison with the Positive Claim in ^{76}Ge," Phys. Rev. Lett. **110**, 062502 (2013), arXiv:1211.3863 [hep-ex].

[9] M. Agostini *et al.* (GERDA), "Results on Neutrinoless Double-β Decay of ^{76}Ge from Phase I of the GERDA Experiment," Phys. Rev. Lett. **111**, 122503 (2013), arXiv:1307.4720 [nucl-ex].

[10] J. B. Albert *et al.* (EXO-200), "Search for Majorana neutrinos with the first two years of EXO-200 data," Nature **510**, 229–234 (2014), arXiv:1402.6956 [nucl-ex].

[11] C. Alduino *et al.* (CUORE), "First Results from CUORE: A Search for Lepton Number Violation via $0\nu\beta\beta$ Decay of ^{130}Te," Phys. Rev. Lett. **120**, 132501 (2018), arXiv:1710.07988 [nucl-ex].

[12] Ke Han (PandaX-III), "PandaX-III: Searching for Neutrinoless Double Beta Decay with High Pressure Gaseous Time Projection Chambers," in *15th International Conference on Topics in Astroparticle and Underground Physics (TAUP 2017) Sudbury, Ontario, Canada, July 24-28, 2017* (2017) arXiv:1710.08908 [physics.ins-det].

[13] O. Azzolini *et al.*, "First Result on the Neutrinoless Double Beta Decay of ^{82}Se with CUPID-0," (2018), arXiv:1802.07791 [nucl-ex].

[14] J. B. Albert *et al.* (EXO), "Search for Neutrinoless Double-Beta Decay with the Upgraded EXO-200 Detector," Phys. Rev. Lett. **120**, 072701 (2018), arXiv:1707.08707 [hep-ex].

[15] K. Alfonso *et al.* (CUORE), "Search for Neutrinoless Double-Beta Decay of ^{130}Te with CUORE-0," Phys. Rev. Lett. **115**, 102502 (2015), arXiv:1504.02454 [nucl-ex].

[16] A. Gando *et al.* (KamLAND-Zen), "Search for Majorana Neutrinos near the Inverted Mass Hierarchy Region with KamLAND-Zen," Phys. Rev. Lett. **117**, 082503 (2016), [Addendum: Phys. Rev. Lett.117,no.10,109903(2016)], arXiv:1605.02889 [hep-ex].

[17] Murray Gell-Mann, Pierre Ramond, and Richard Slansky, "Complex Spinors and Unified Theories," *Supergravity Workshop Stony Brook, New York, September 27-28, 1979*, Conf. Proc. **C790927**, 315–321 (1979), arXiv:1306.4669 [hep-th].

[18] Tsutomu Yanagida, "HORIZONTAL SYMMETRY AND MASSES OF NEUTRINOS," *Proceedings: Workshop on the Unified Theories and the Baryon Number in the Universe: Tsukuba, Japan, February 13-14, 1979*, Conf. Proc. **C7902131**, 95–99 (1979).

[19] S. L. Glashow, "The future of elementary particle physics," in *Quarks and Leptons*, edited by Maurice Lévy, Jean-Louis Basdevant, David Speiser, Jacques Weyers, Raymond Gastmans, and Maurice Jacob (Springer US, Boston, MA, 1980) pp. 687–713.

[20] Rabindra N. Mohapatra and Goran Senjanović, "Neutrino mass and spontaneous parity nonconservation," Phys. Rev. Lett. **44**, 912–915 (1980).

[21] Pierre Ramond, "The Family Group in Grand Unified Theories," in *International Symposium on Fundamentals of Quantum Theory and Quantum Field Theory Palm Coast, Florida, February 25-March 2, 1979* (1979) pp. 265–280, arXiv:hep-ph/9809459 [hep-ph].

[22] Gary Prezeau, M. Ramsey-Musolf, and Petr Vogel, "Neutrinoless double beta decay and effective field theory," Phys. Rev. **D68**, 034016 (2003), arXiv:hep-ph/0303205.

[23] Michael L. Graesser, "An electroweak basis for neutrinoless double β decay," JHEP **08**, 099 (2017), arXiv:1606.04549 [hep-ph].

[24] G. Peter Lepage, "The Analysis of Algorithms for Lattice Field Theory," , 97–120 (1989).

[25] Laurent Lellouch and Martin Luscher, "Weak transition matrix elements from finite volume correlation functions," Commun.Math.Phys. **219**, 31–44 (2001), arXiv:hep-lat/0003023 [hep-lat].

[26] Raúl A. Briceño and Maxwell T. Hansen, "Relativistic, model-independent, multichannel $2 \to 2$ transition amplitudes in a finite volume," Phys. Rev. **D94**, 013008 (2016), arXiv:arXiv:1509.08507 [hep-lat].

[27] Y. Takahashi, "The Fierz Identities," in *Progress in Quantum Field Theory*, edited by H. Ezawa and S. Kamefuchi (North-Holland, Amsterdam, 1986) p. 121.

[28] A. Bazavov *et al.* (MILC), "Lattice QCD ensembles with four flavors of highly improved staggered quarks," Phys. Rev. **D87**, 054505 (2013), arXiv:arXiv:1212.4768 [hep-lat].

[29] A. Bazavov *et al.* (MILC), "Gradient flow and scale setting on MILC HISQ ensembles," Phys. Rev. **D93**, 094510 (2016), arXiv:arXiv:1503.02769 [hep-lat].

[30] Richard C. Brower, Hartmut Neff, and Kostas Orginos, "Mobius fermions: Improved domain wall chiral fermions," *Lattice field theory. Proceedings, 22nd International Symposium, Lattice 2004, Batavia, USA, June 21-26, 2004*, Nucl. Phys. Proc. Suppl. **140**, 686–688 (2005), [,686(2004)], arXiv:hep-lat/0409118 [hep-lat].

[31] R. C. Brower, H. Neff, and K. Orginos, "Mobius fermions," *Hadron physics, proceedings of the Workshop on Computational Hadron Physics, University of Cyprus, Nicosia, Cyprus, 14-17 September 2005*, Nucl. Phys. Proc. Suppl. **153**, 191–198 (2006), arXiv:hep-lat/0511031 [hep-lat].

[32] Richard C. Brower, Harmut Neff, and Kostas Orginos, "The Möbius domain wall fermion algorithm," Comput. Phys. Commun. **220**, 1–19 (2017), arXiv:1206.5214 [hep-lat].

[33] R. Narayanan and H. Neuberger, "Infinite N phase transitions in continuum Wilson loop operators," JHEP **03**, 064 (2006), arXiv:hep-th/0601210 [hep-th].

[34] Martin Luscher and Peter Weisz, "Perturbative analysis of the gradient flow in non-abelian gauge theories," JHEP **02**, 051 (2011), arXiv:1101.0963 [hep-th].

[35] Martin Luscher, "Chiral symmetry and the Yang–Mills gradient flow," JHEP **04**, 123 (2013), arXiv:1302.5246 [hep-lat].

[36] E. Berkowitz, C. Bouchard, C.C Chang, M.A. Clark, B Joo, T. Kurth, C. Monahan, A. Nicholson, K. Orginos, E. Rinaldi, P. Vranas, and A. Walker-Loud, "Möbius Domain-Wall fermions on gradient-flowed dynamical HISQ ensembles," Phys. Rev. **D96**, 054513 (2017), arXiv:1701.07559 [hep-lat].

[37] E. Berkowitz, C. Bouchard, D. B. Brantley, C.C Chang, M.A. Clark, N. Garron, B Joó, T. Kurth, C. Monahan, H. Monge-Camacho, A. Nicholson, K. Orginos, E. Rinaldi, P. Vranas, and A. Walker-Loud, "An accurate calculation of the nucleon axial charge with lattice QCD," (2017), arXiv:1704.01114 [hep-lat].

[38] C.C Chang, A. Nicholson, E. Rinaldi, E. Berkowitz, N. Garron, D. B. Brantley, H. Monge-Camacho, C. Monahan, C. Bouchard, M.A. Clark, B Joó, T. Kurth, K. Orginos, P. Vranas, and A. Walker-Loud, "Nucleon axial coupling from Lattice QCD," in *35th International Symposium on Lattice Field Theory (Lattice 2017) Granada, Spain, June 18-24, 2017* (2017) arXiv:1710.06523 [hep-lat].

[39] C.C Chang, A. Nicholson, E. Rinaldi, E. Berkowitz, N. Garron, D. B. Brantley, H. Monge-Camacho, C. Monahan, C. Bouchard, M.A. Clark, B Joó, T. Kurth, K. Orginos, P. Vranas, and A. Walker-Loud, "A percent-level determination of the nucleon axial coupling from Quantum Chromodynamics," (2018), Accepted for publication.
[40] Y. Aoki *et al.*, "Continuum Limit of B_K from 2+1 Flavor Domain Wall QCD," Phys. Rev. **D84**, 014503 (2011), arXiv:1012.4178 [hep-lat].
[41] S. Durr *et al.*, "Precision computation of the kaon bag parameter," Phys. Lett. **B705**, 477–481 (2011), arXiv:1106.3230 [hep-lat].
[42] P. A. Boyle, N. Garron, and R. J. Hudspith (RBC, UKQCD), "Neutral kaon mixing beyond the standard model with $n_f = 2+1$ chiral fermions," Phys. Rev. **D86**, 054028 (2012), arXiv:1206.5737 [hep-lat].
[43] V. Bertone *et al.* (ETM), "Kaon Mixing Beyond the SM from N$_f$=2 tmQCD and model independent constraints from the UTA," JHEP **03**, 089 (2013), [Erratum: JHEP07,143(2013)], arXiv:1207.1287 [hep-lat].
[44] Taegil Bae *et al.* (SWME), "Neutral kaon mixing from new physics: matrix elements in $N_f = 2+1$ lattice QCD," Phys. Rev. **D88**, 071503 (2013), arXiv:1309.2040 [hep-lat].
[45] Taegil Bae *et al.* (SWME), "Improved determination of BK with staggered quarks," Phys. Rev. **D89**, 074504 (2014), arXiv:1402.0048 [hep-lat].
[46] N. Carrasco, P. Dimopoulos, R. Frezzotti, V. Lubicz, G. C Rossi, S. Simula, and C. Tarantino (ETM), "S=2 and C=2 bag parameters in the standard model and beyond from N$_f$=2+1+1 twisted-mass lattice QCD," Phys. Rev. **D92**, 034516 (2015), arXiv:1505.06639 [hep-lat].
[47] Benjamin J. Choi *et al.* (SWME), "Kaon BSM B-parameters using improved staggered fermions from $N_f = 2+1$ unquenched QCD," Phys. Rev. **D93**, 014511 (2016), arXiv:1509.00592 [hep-lat].
[48] Nicolas Garron, Renwick J. Hudspith, and Andrew T. Lytle (RBC/UKQCD), "Neutral Kaon Mixing Beyond the Standard Model with $n_f = 2+1$ Chiral Fermions Part 1: Bare Matrix Elements and Physical Results," JHEP **11**, 001 (2016), arXiv:1609.03334 [hep-lat].
[49] A. Bazavov *et al.*, "Short-distance matrix elements for D^0-meson mixing for $N_f = 2+1$ lattice QCD," Phys. Rev. **D97**, 034513 (2018), arXiv:1706.04622 [hep-lat].
[50] Elvira Gamiz, Christine T. H. Davies, G. Peter Lepage, Junko Shigemitsu, and Matthew Wingate (HPQCD), "Neutral B Meson Mixing in Unquenched Lattice QCD," Phys. Rev. **D80**, 014503 (2009), arXiv:0902.1815 [hep-lat].
[51] N. Carrasco *et al.* (ETM), "B-physics from $N_f = 2$ tmQCD: the Standard Model and beyond," JHEP **03**, 016 (2014), arXiv:1308.1851 [hep-lat].
[52] Yasumichi Aoki, Tomomi Ishikawa, Taku Izubuchi, Christoph Lehner, and Amarjit Soni, "Neutral B meson mixings and B meson decay constants with static heavy and domain-wall light quarks," Phys. Rev. **D91**, 114505 (2015), arXiv:1406.6192 [hep-lat].
[53] A. Bazavov *et al.* (Fermilab Lattice, MILC), "$B^0_{(s)}$-mixing matrix elements from lattice QCD for the Standard Model and beyond," Phys. Rev. **D93**, 113016 (2016), arXiv:1602.03560 [hep-lat].
[54] Michael I. Buchoff, Chris Schroeder, and Joseph Wasem, "Neutron-antineutron oscillations on the lattice," PoS **LATTICE2012**, 128 (2012), arXiv:1207.3832 [hep-lat].
[55] Sergey Syritsyn, Michael I. Buchoff, Chris Schroeder, and Joseph Wasem, "Neutron-Antineutron Oscillation Matrix Elements with Domain Wall Fermions at the Physical Point," *Proceedings, 33rd International Symposium on Lattice Field Theory (Lattice 2015)*, PoS **LATTICE2015**, 132 (2015).
[56] Amy Nicholson, Evan Berkowitz, Chia Cheng Chang, M. A. Clark, Balint Joo, Thorsten Kurth, Enrico Rinaldi, Brian Tiburzi, Pavlos Vranas, and Andre Walker-Loud, "Neutrinoless double beta decay from lattice QCD," *Proceedings, 34th International Symposium on Lattice Field Theory (Lattice 2016): Southampton, UK, July 24-30, 2016*, PoS **LATTICE2016**, 017 (2016), arXiv:1608.04793 [hep-lat].
[57] J. Gasser and H. Leutwyler, "Chiral Perturbation Theory to One Loop," Annals Phys. **158**, 142 (1984).
[58] Stephen R. Sharpe and Robert L. Singleton, Jr, "Spontaneous flavor and parity breaking with Wilson fermions," Phys. Rev. **D58**, 074501 (1998), arXiv:hep-lat/9804028 [hep-lat].
[59] J. Gasser and H. Leutwyler, "Spontaneously Broken Symmetries: Effective Lagrangians at Finite Volume," Nucl. Phys. **B307**, 763–778 (1988).
[60] G. Martinelli, C. Pittori, Christopher T. Sachrajda, M. Testa, and A. Vladikas, "A General method for nonperturbative renormalization of lattice operators," Nucl. Phys. **B445**, 81–108 (1995), arXiv:hep-lat/9411010.
[61] C. Sturm, Y. Aoki, N.H. Christ, T. Izubuchi, C.T.C. Sachrajda, *et al.*, "Renormalization of quark bilinear operators in a momentum-subtraction scheme with a nonexceptional subtraction point," Phys.Rev. **D80**, 014501 (2009), arXiv:0901.2599 [hep-ph].
[62] Peter A. Boyle, Nicolas Garron, Renwick J. Hudspith, Christoph Lehner, and Andrew T. Lytle (RBC, UKQCD), "Neutral kaon mixing beyond the Standard Model with n$_f = 2+1$ chiral fermions. Part 2: non perturbative renormalisation of the $\Delta F = 2$ four-quark operators," JHEP **10**, 054 (2017), arXiv:1708.03552 [hep-lat].
[63] M. Gockeler, R. Horsley, H. Oelrich, H. Perlt, D. Petters, *et al.*, "Nonperturbative renormalization of composite operators in lattice QCD," Nucl.Phys. **B544**, 699–733 (1999), arXiv:hep-lat/9807044 [hep-lat].
[64] R. Arthur and P.A. Boyle (RBC/UKQCD), "Step Scaling with off-shell renormalisation," Phys.Rev. **D83**, 114511 (2011), arXiv:1006.0422 [hep-lat].
[65] R. Arthur, P.A. Boyle, N. Garron, C. Kelly, and A.T. Lytle (RBC/UKQCD), "Opening the Rome-Southampton window for operator mixing matrices," Phys.Rev. **D85**, 014501 (2012), arXiv:1109.1223 [hep-lat].
[66] CalLat, "`project_0vbb`," (2018).
[67] G. Peter Lepage, "`lsqfit` v9.3," (2018).
[68] V. Cirigliano, W. Dekens, M. Graesser, and E. Mereghetti, "Neutrinoless double beta decay and chiral $SU(3)$," Phys. Lett. **B769**, 460–464 (2017), arXiv:1701.01443 [hep-ph].
[69] A. Pich and E. De Rafael, "K anti-K Mixing in the Standard Model," Phys. Lett. **158B**, 477–484 (1985).
[70] Antonio Pich and Eduardo de Rafael, "Four quark operators and nonleptonic weak transitions," Nucl. Phys.

B358, 311–382 (1991).
[71] Santiago Peris and Eduardo de Rafael, "K0 anti-K0 mixing in the 1 / N(c) expansion," Phys. Lett. **B490**, 213–222 (2000), arXiv:hep-ph/0006146 [hep-ph].
[72] H. Päs, M. Hirsch, H.V. Klapdor-Kleingrothaus, and S.G. Kovalenko, "Towards a superformula for neutrinoless double beta decay," Physics Letters B **453**, 194 – 198 (1999).
[73] H. Pas, M. Hirsch, H. V. Klapdor-Kleingrothaus, and S. G. Kovalenko, "A Superformula for neutrinoless double beta decay. 2. The Short range part," Phys. Lett. **B498**, 35–39 (2001), arXiv:hep-ph/0008182 [hep-ph].
[74] Werner Rodejohann, "Neutrino-less Double Beta Decay and Particle Physics," Int. J. Mod. Phys. **E20**, 1833–1930 (2011), arXiv:1106.1334 [hep-ph].
[75] Tao Peng, Michael J. Ramsey-Musolf, and Peter Winslow, "TeV lepton number violation: From neutrinoless double-β decay to the LHC," Phys. Rev. **D93**, 093002 (2016), arXiv:1508.04444 [hep-ph].
[76] Shao-Feng Ge, Manfred Lindner, and Sudhanwa Patra, "New physics effects on neutrinoless double beta decay from right-handed current," JHEP **10**, 077 (2015), arXiv:1508.07286 [hep-ph].
[77] Jonathan Engel and Javier Menéndez, "Status and Future of Nuclear Matrix Elements for Neutrinoless Double-Beta Decay: A Review," Rept. Prog. Phys. **80**, 046301 (2017), arXiv:1610.06548 [nucl-th].
[78] Fahim Ahmed, Andrei Neacsu, and Mihai Horoi, "Interference between light and heavy neutrinos for $0\nu\beta\beta$ decay in the left?right symmetric model," Phys. Lett. **B769**, 299–304 (2017), arXiv:1701.03177 [hep-ph].
[79] Mihai Horoi and Andrei Neacsu, "Towards an effective field theory approach to the neutrinoless double-beta decay," (2017), arXiv:1706.05391 [hep-ph].
[80] V. Cirigliano, W. Dekens, J. de Vries, M. L. Graesser, and E. Mereghetti, "Neutrinoless double beta decay in chiral effective field theory: lepton number violation at dimension seven," JHEP **12**, 082 (2017), arXiv:1708.09390 [hep-ph].
[81] J. Menéndez, "Neutrinoless $\beta\beta$ decay mediated by the exchange of light and heavy neutrinos: The role of nuclear structure correlations," J. Phys. **G45**, 014003 (2018), arXiv:1804.02105 [nucl-th].
[82] M. González, M. Hirsch, and S. G. Kovalenko, "QCD running in neutrinoless double beta decay: Short-range mechanisms," Phys. Rev. **D93**, 013017 (2016), arXiv:1511.03945 [hep-ph].
[83] Vincenzo Cirigliano, Wouter Dekens, Jordy De Vries, Michael L. Graesser, Emanuele Mereghetti, Saori Pastore, and Ubirajara Van Kolck, "A new leading contribution to neutrinoless double-beta decay," (2018), arXiv:1802.10097 [hep-ph].
[84] Thorsten Kurth, Evan Berkowitz, Enrico Rinaldi, Pavlos Vranas, Amy Nicholson, Mark Strother, and Andre Walker-Loud, "Nuclear Parity Violation from Lattice QCD," *Proceedings, 33rd International Symposium on Lattice Field Theory (Lattice 2015)*, PoS **LATTICE2015**, 329 (2015), arXiv:1511.02260 [hep-lat].
[85] Martin J. Savage, Phiala E. Shanahan, Brian C. Tiburzi, Michael L. Wagman, Frank Winter, Silas R. Beane, Emmanuel Chang, Zohreh Davoudi, William Detmold, and Kostas Orginos, "Axial-Current Matrix Elements in Light Nuclei from Lattice QCD," *Proceedings, 38th International Conference on High Energy Physics (ICHEP 2016): Chicago, IL, USA, August 3-10, 2016*, PoS **ICHEP2016**, 506 (2016), arXiv:1611.00344 [hep-lat].
[86] Martin J. Savage, Phiala E. Shanahan, Brian C. Tiburzi, Michael L. Wagman, Frank Winter, Silas R. Beane, Emmanuel Chang, Zohreh Davoudi, William Detmold, and Kostas Orginos, "Proton-Proton Fusion and Tritium β Decay from Lattice Quantum Chromodynamics," Phys. Rev. Lett. **119**, 062002 (2017), arXiv:1610.04545 [hep-lat].
[87] Emmanuel Chang, Zohreh Davoudi, William Detmold, Arjun S. Gambhir, Kostas Orginos, Martin J. Savage, Phiala E. Shanahan, Michael L. Wagman, and Frank Winter, "Nuclear modification of scalar, axial and tensor charges from lattice QCD," Phys. Rev. Lett. **120**, 152002 (2018), arXiv:1712.03221 [hep-lat].
[88] Brian C. Tiburzi, Michael L. Wagman, Frank Winter, Emmanuel Chang, Zohreh Davoudi, William Detmold, Kostas Orginos, Martin J. Savage, and Phiala E. Shanahan, "Double-β Decay Matrix Elements from Lattice Quantum Chromodynamics," Phys. Rev. **D96**, 054505 (2017), arXiv:1702.02929 [hep-lat].
[89] Phiala E. Shanahan, Brian C. Tiburzi, Michael L. Wagman, Frank Winter, Emmanuel Chang, Zohreh Davoudi, William Detmold, Kostas Orginos, and Martin J. Savage, "Isotensor Axial Polarizability and Lattice QCD Input for Nuclear Double-β Decay Phenomenology," Phys. Rev. Lett. **119**, 062003 (2017), arXiv:1701.03456 [hep-lat].
[90] Robert G. Edwards and Balint Joo (SciDAC, LHPC, UKQCD), "The Chroma software system for lattice QCD," *Lattice field theory. Proceedings, 22nd International Symposium, Lattice 2004, Batavia, USA, June 21-26, 2004*, Nucl. Phys. Proc. Suppl. **140**, 832 (2005), [,832(2004)], arXiv:hep-lat/0409003 [hep-lat].
[91] M. A. Clark, R. Babich, K. Barros, R. C. Brower, and C. Rebbi, "Solving Lattice QCD systems of equations using mixed precision solvers on GPUs," Comput. Phys. Commun. **181**, 1517–1528 (2010), arXiv:0911.3191 [hep-lat].
[92] R. Babich, M. A. Clark, B. Joo, G. Shi, R. C. Brower, and S. Gottlieb, "Scaling Lattice QCD beyond 100 GPUs," in *SC11 International Conference for High Performance Computing, Networking, Storage and Analysis Seattle, Washington, November 12-18, 2011* (2011) arXiv:1109.2935 [hep-lat].
[93] Evan Berkowitz, "METAQ: Bundle Supercomputing Tasks," (2017), `https://github.com/evanberkowitz/metaq`, arXiv:1702.06122 [physics.comp-ph].
[94] C.C Chang, A. Nicholson, E. Rinaldi, E. Berkowitz, N. Garron, D. B. Brantley, H. Monge-Camacho, C. Monahan, C. Bouchard, M.A. Clark, B Joó, T. Kurth, K. Orginos, P. Vranas, and A. Walker-Loud, "A percent-level determination of the nucleon axial coupling from Quantum Chromodynamcis," .
[95] Andrzej J. Buras, Mikolaj Misiak, and Jorg Urban, "Two loop QCD anomalous dimensions of flavor changing four quark operators within and beyond the standard model," Nucl. Phys. **B586**, 397–426 (2000), arXiv:hep-ph/0005183 [hep-ph].
[96] T. van Ritbergen, J. A. M. Vermaseren, and S. A. Larin, "The Four loop beta function in quantum chromodynamics," Phys. Lett. **B400**, 379–384 (1997), arXiv:hep-ph/9701390 [hep-ph].
[97] K. G. Chetyrkin, Bernd A. Kniehl, and M. Steinhauser,

"Strong coupling constant with flavor thresholds at four loops in the MS scheme," Phys. Rev. Lett. **79**, 2184–2187 (1997), arXiv:hep-ph/9706430 [hep-ph].

[98] Oliver Bar, Gautam Rupak, and Noam Shoresh, "Simulations with different lattice Dirac operators for valence and sea quarks," Phys. Rev. **D67**, 114505 (2003), arXiv:hep-lat/0210050 [hep-lat].

[99] Oliver Bar, Gautam Rupak, and Noam Shoresh, "Chiral perturbation theory at O(a**2) for lattice QCD," Phys. Rev. **D70**, 034508 (2004), arXiv:hep-lat/0306021 [hep-lat].

[100] Brian C. Tiburzi, "Baryon masses at O(a**2) in chiral perturbation theory," Nucl. Phys. **A761**, 232–258 (2005), arXiv:hep-lat/0501020 [hep-lat].

[101] Oliver Bar, Claude Bernard, Gautam Rupak, and Noam Shoresh, "Chiral perturbation theory for staggered sea quarks and Ginsparg-Wilson valence quarks," Phys. Rev. **D72**, 054502 (2005), arXiv:hep-lat/0503009 [hep-lat].

[102] Brian C. Tiburzi, "Baryons with Ginsparg-Wilson quarks in a staggered sea," Phys. Rev. **D72**, 094501 (2005), [Erratum: Phys. Rev.D79,039904(2009)], arXiv:hep-lat/0508019 [hep-lat].

[103] Jiunn-Wei Chen, Donal O'Connell, Ruth S. Van de Water, and Andre Walker-Loud, "Ginsparg-Wilson pions scattering on a staggered sea," Phys. Rev. **D73**, 074510 (2006), arXiv:hep-lat/0510024 [hep-lat].

[104] Jiunn-Wei Chen, Donal O'Connell, and Andre Walker-Loud, "Two Meson Systems with Ginsparg-Wilson Valence Quarks," Phys. Rev. **D75**, 054501 (2007), arXiv:hep-lat/0611003 [hep-lat].

[105] Jiunn-Wei Chen, Donal O'Connell, and Andre Walker-Loud, "Universality of mixed action extrapolation formulae," JHEP **04**, 090 (2009), arXiv:0706.0035 [hep-lat].

[106] Jiunn-Wei Chen, Maarten Golterman, Donal O'Connell, and Andre Walker-Loud, "Mixed Action Effective Field Theory: An Addendum," Phys. Rev. **D79**, 117502 (2009), arXiv:0905.2566 [hep-lat].

[107] Claude W. Bernard and Maarten F. L. Golterman, "Partially quenched gauge theories and an application to staggered fermions," Phys. Rev. **D49**, 486–494 (1994), arXiv:hep-lat/9306005 [hep-lat].

[108] Stephen R. Sharpe, "Enhanced chiral logarithms in partially quenched QCD," Phys. Rev. **D56**, 7052–7058 (1997), [Erratum: Phys. Rev.D62,099901(2000)], arXiv:hep-lat/9707018 [hep-lat].

[109] Stephen R. Sharpe and Noam Shoresh, "Physical results from unphysical simulations," Phys. Rev. **D62**, 094503 (2000), arXiv:hep-lat/0006017 [hep-lat].

[110] Stephen R. Sharpe and Noam Shoresh, "Partially quenched chiral perturbation theory without Phi0," Phys. Rev. **D64**, 114510 (2001), arXiv:hep-lat/0108003 [hep-lat].

[111] Claude Bernard and Maarten Golterman, "On the foundations of partially quenched chiral perturbation theory," Phys. Rev. **D88**, 014004 (2013), arXiv:1304.1948 [hep-lat].

[112] J. Noaki *et al.* (TWQCD, JLQCD), "Convergence of the chiral expansion in two-flavor lattice QCD," Phys. Rev. Lett. **101**, 202004 (2008), arXiv:0806.0894 [hep-lat].

[113] S. Aoki *et al.*, "Review of lattice results concerning low-energy particle physics," Eur. Phys. J. **C77**, 112 (2017), arXiv:1607.00299 [hep-lat].

[114] Szabolcs Borsanyi *et al.*, "High-precision scale setting in lattice QCD," JHEP **09**, 010 (2012), arXiv:1203.4469 [hep-lat].

Non-perturbative renormalization

The complete details of our renormalization procedure will be presented in a forthcoming publication. Here, we summarize the pertinent details. As discussed in the main text, we used a RI/SMOM scheme with $\mu^2 \equiv p_{in}^2 = p_{out}^2 = (p_{out} - p_{in})^2$ as proposed in [61]. This choice of momentum suppresses infrared (IR) contamination which arises, for example, from light pion exchanges and can induce unphysical mixing of operators of different chirality. Although in principle such IR effects can still be present, they are expected to be sub-leading if we keep the renormalization scale μ high enough, eg. $\mu^2 \gg m_\pi^2, \Lambda_{QCD}^2$. In practice we check that $Z_A = Z_V, Z_P = Z_S$ and that the chirally forbidden matrix elements of the four-quark operators are orders of magnitude smaller than the allowed matrix elements.

Both the renormalized operators and their respective matrix elements are determined in a renormalization scheme R

$$\mathcal{O}_i^R = Z_{ij}^R \mathcal{O}_j^{latt}\,, \tag{10}$$

where $\mathcal{O}^{latt}$ are the bare matrix elements determined by analyzing the ratio correlation functions, Eq. (3), which are provided with our Jupyter notebook [66].

In order to determine the renormalization matrix, Z^R, on Landau-fixed gauge configurations, we compute Π_i, the amputated vertex functions of the operators $\mathcal{O}_i$ given in Eq. (1) with the aforementioned SMOM kinematics (see for example, Eq.(15) of Ref. [62]). The renormalization factors are determined by first analyzing a matrix of projected amputated vertex functions $\Lambda_{ij} = P_j\,[\Pi_i]$ as a function of μ and the light quark mass. For convenience, we normalize this matrix by Λ_V^2, where Λ_V is the corresponding amputated-projected Green function for the local vector current. After extrapolating the vertex functions to the chiral limit, the renormalization matrix is related to the inverse of Λ:

$$\frac{Z^a(\mu)}{(Z_V^a)^2}\Lambda(\mu, a) = F\,, \tag{11}$$

where F is the corresponding free-field matrix. The projectors P and the matrix F are given in [62].

The direct computation of the renormalization factors on our coarsest ensemble, $a \sim 0.15$ fm, likely suffers from large discretization effects. To circumvent this problem, a non-perturbative step-scaling function is determined by performing a simultaneous fit in the lattice spacing, a and the renormalization scale μ,

$$\Sigma_{ij}(\mu_2, \mu_1, a) \equiv \Lambda_{ii'}^{-1}(\mu_2, a)\Lambda_{i'j}(\mu_1, a)\,. \tag{12}$$

We then determine a continuum step-scaling function,

$$\sigma_{ij}(\mu_2, \mu_1) \equiv \lim_{a\to 0} \Sigma_{ij}(\mu_2, \mu_1, a)\,. \tag{13}$$

On the coarsest ensemble, we keep the largest values of μ_2 used in the determination of this continuum step-scaling function sufficiently small that we observe it is insensitive to the largest value used. We perform a similar study on the $a \sim 0.12$ fm ensembles and find the largest value of μ_2 on this ensemble can be taken larger than 3 GeV.

The continuum step-scaling function, Eq. (13), is then used to raise the renormalization matrices on all ensembles from $\mu_1 = 2$ GeV to $\mu_2 = 3$ GeV,

$$\frac{Z_{ij}^a(\mu_2)}{(Z_V^a)^2} = \sigma_{ii'}(\mu_2, \mu_1)\frac{Z_{i'j}^a(\mu_1)}{(Z_V^a)^2}\,. \tag{14}$$

Finally, the values of Z_V are determined from the relation $Z_V g_V = 1$. The values of g_V in the supplemental material Table 1 of Ref. [94] are extrapolated to the chiral limit for each lattice spacing to determine the values of Z_V^a which are then used to determine

$$Z^a(\mu) = \frac{Z^a(\mu)}{(Z_V^a)^2}(Z_V^a)^2\,. \tag{15}$$

Using the following operators order

$$\mathcal{O}^T = \{\mathcal{O}_1^{++}, \mathcal{O}_1'^{++}, \mathcal{O}_2^{++}, \mathcal{O}_2'^{++}, \mathcal{O}_3^{++}\}\,, \tag{16}$$

the renormalization matrices Z^a in the RI/SMOM scheme at $\mu = 3$ GeV are given by

$$Z^{\rm a15}(\mu = 3\text{ GeV}) = \begin{pmatrix} 0.9835(68) & -0.0106(18) & 0 & 0 & 0 \\ -0.0369(30) & 1.0519(80) & 0 & 0 & 0 \\ 0 & 0 & 1.020(11) & -0.0356(49) & 0 \\ 0 & 0 & -0.0485(31) & 0.9519(68) & 0 \\ 0 & 0 & 0 & 0 & 0.9407(63) \end{pmatrix}$$

$$Z^{\rm a12}(\mu = 3\text{ GeV}) = \begin{pmatrix} 0.9535(48) & -0.0130(17) & 0 & 0 & 0 \\ -0.0284(30) & 0.9922(60) & 0 & 0 & 0 \\ 0 & 0 & 0.9656(96) & -0.0275(49) & 0 \\ 0 & 0 & -0.0360(28) & 0.9270(50) & 0 \\ 0 & 0 & 0 & 0 & 0.9117(43) \end{pmatrix}$$

$$Z^{\text{a09}}(\mu = 3\text{ GeV}) = \begin{pmatrix} 0.9483(44) & -0.0269(17) & 0 & 0 & 0 \\ -0.0236(29) & 0.9369(54) & 0 & 0 & 0 \\ 0 & 0 & 0.9209(91) & -0.0224(49) & 0 \\ 0 & 0 & -0.0230(28) & 0.9332(47) & 0 \\ 0 & 0 & 0 & 0 & 0.9017(39) \end{pmatrix} \quad (17)$$

We also convert these Z matrices to the $\overline{\text{MS}}$ scheme defined in [95] to provide our final matrix elements in both schemes. To obtain the value of the strong coupling, we start from $\alpha_S(m_Z) = 0.1182$, using the four-loop β-function of [96, 97] and adapting the number of flavors while crossing the b-threshold, we find $\alpha_S(\mu) = 0.2541$ at $\mu = 3$ GeV in the $N_f = 4$ theory. We then use the one-loop matching coefficients given in [62] for the SMOM-(γ_μ, γ_μ) scheme and obtain the matrix R: defining R as $\mathcal{O}^{\overline{\text{MS}}} = R\mathcal{O}^{RI/SMOM}$ with $\mathcal{O}^T = \{\mathcal{O}_1, \mathcal{O}_1', \mathcal{O}_2, \mathcal{O}_2', \mathcal{O}_3\}$, for $\mu = 3$ GeV in both schemes, R is given by

$$R = \begin{pmatrix} 1.0009 & -0.0026 & 0 & 0 & 0 \\ -0.0326 & 1.0909 & 0 & 0 & 0 \\ 0 & 0 & 1.0308 & 0.0201 & 0 \\ 0 & 0 & 0.0135 & 1.1060 & 0 \\ 0 & 0 & 0 & 0 & 1.0043 \end{pmatrix} \quad (18)$$

up to $O(\alpha_S^2)$ terms.

The bare matrix elements in lattice units are provided with our Jupyter notebook [66]. To convert these values to into physical units, they are multiplied by the corresponding renormalization matrix from Eq. (17), and converted to physical units using the values of a/w_0 and w_0 given in Ref. [29].

Derivation of extrapolation formulae

The formula used to perform the chiral, continuum and infinite volume extrapolations, Eqs. (41)–(43), can be derived with mixed-action effective field theory (MAEFT) [98–106]. At one-loop order, MAEFT extrapolation formulas can be directly determined from their respective partially quenched χPT (PQχPT) [107–111] expressions [105].

The set of dimension-9 operators considered in this work, Eqs. (1) and (2), were first derived in Ref. [22]. When constructing the operators in the chiral Lagrangian, as noted in Ref. [22], the color mixed and unmixed operators transform in the same way under chiral transformations, and so they do not give rise to distinguishable operators at the hadronic level. Under $SU(2)$ chiral transformations, the operators transform as

$$\mathcal{O}_{1+}^{++} \sim \tau_L^+ \otimes \tau_R^+ \,,$$
$$\mathcal{O}_{2+}^{++} \sim \tau_{RL}^+ \otimes \tau_{RL}^+ + \tau_{LR}^+ \otimes \tau_{LR}^+ \,,$$
$$\mathcal{O}_{3+}^{++} \sim \tau_L^+ \otimes \tau_L^+ + \tau_R^+ \otimes \tau_R^+ \,, \quad (19)$$

with similar transformation properties for the two color-mixed operators respectively. The $\tau_L^+, \tau_R^+, \tau_{RL}^+$ are spurion operators transforming as

$$\begin{aligned} \tau_L^+ &\to L\tau_L^+ L^\dagger \,, \\ \tau_R^+ &\to R\tau_R^+ R^\dagger \,, \\ \tau_{LR}^+ &\to L\tau_{LR}^+ R^\dagger \,, \\ \tau_{RL}^+ &\to R\tau_{RL}^+ L^\dagger \,. \end{aligned} \quad (20)$$

They are set to the raising operator

$$\tau^+ = \begin{pmatrix} 0 & 1 \\ 0 & 0 \end{pmatrix} \,, \quad (21)$$

to compute the various $\pi^- \to \pi^+$ transition amplitudes.

Following closely the power-counting arguments discussed Ref. [22], the low-energy operators in the chiral Lagrangian that give rise to these $\pi^- \to \pi^+ e^- e^-$ operators are

$$\mathcal{L}^\chi = \bar{e}e^c \frac{G_F^2}{\Lambda_{\beta\beta}} \frac{\Lambda_{\chi_0}^4}{(4\pi)^2} \frac{F^2}{4} \Big[c_1^W \beta_1 \mathcal{O}_{1+}^\chi - c_2^W \frac{\beta_2}{2} \mathcal{O}_{2+}^\chi - c_3^W \beta_3 \mathcal{O}_{3+}^\chi \Big] \,. \quad (22)$$

In this Lagrangian, G_F is Fermi's weak decay constant, $\Lambda_{\beta\beta}$ is the ultraviolet scale associated with the new, lepton number violating, physics. The chiral symmetry breaking scale is $\Lambda_{\chi_0} = 4\pi F$ where F is the pion decay constant in the chiral limit with normalization $F_\pi^{phys} \simeq 92.2$ MeV. The Wilson coefficients, c_i^W, arise from integrating out heavy BSM physics and matching to the local Lagrangian in terms of SM fields. The β_i are dimensionless low-energy constants (LECs) which must be determined to predict the strength of the various $\pi^- \to \pi^+$ transition operators. The prefactors and signs were chosen such that the leading order hadronic contribution to each matrix element is simply given by $\beta_i \Lambda_\chi^4/(4\pi)^2$.

At the quark level, the $\langle \pi | \mathcal{O}_{i+}^{++} | \pi \rangle$ matrix elements have mass dimension four. At the hadronic level, the pion fields are parameterized by the dimensionless Σ field and so the mass dimensions of the matrix element are manifested in terms of hadronic scales, $\Lambda_{\chi_0}^4/(4\pi)^2$. The dimensionless hadronic operators are given by

$$\mathcal{O}_{1+}^\chi = \text{Tr}\left(\Sigma^\dagger \tau_L^+ \Sigma \tau_R^+\right) \,, \quad (23)$$

$$\mathcal{O}^{\chi}_{2+} = \text{Tr}\left(\Sigma^\dagger \tau^+_{LR}\Sigma^\dagger\tau^+_{LR} + \Sigma\tau^+_{RL}\Sigma\tau^+_{RL}\right) \,, \quad (24)$$

$$\mathcal{O}^{\chi}_{3+} = \frac{1}{\Lambda^2_{\chi_0}}\text{Tr}\left(\Sigma_{L\mu}\tau^+_L\Sigma^\mu_L\tau^+_L + \Sigma_{R\mu}\tau^+_R\Sigma^\mu_R\tau^+_R\right) \,, \quad (25)$$

with identical operators for the $\mathcal{O}'^{++}_{1,2}$ quark level operators. At the hadronic level, the only difference in color mixed and unmixed operators is the value of the LECs, β_i. The pions are parameterized in the Σ fields

$$\xi^2 = \Sigma = e^{\sqrt{2}i\phi/F} \quad (26)$$

with

$$\phi = \begin{pmatrix} \frac{\pi^0}{\sqrt{2}} & \pi^+ \\ \pi^- & -\frac{\pi^0}{\sqrt{2}} \,, \end{pmatrix} \quad (27)$$

and

$$\Sigma^\mu_L = \Sigma\partial^\mu\Sigma^\dagger \,,$$
$$\Sigma^\mu_R = \Sigma^\dagger\partial^\mu\Sigma \,. \quad (28)$$

In order to renormalize the loop integrals appearing at next-to-leading order in the chiral expansion, we need higher dimensional operators to serve as counterterms. Using the LO equations of motion to eliminate redundant operators, the hadronic component of the operators are given by

$$\mathcal{O}^{nlo}_{1+} = \frac{\text{Tr}\left(\partial_\mu\Sigma^\dagger\tau^+_L\partial^\mu\Sigma\tau^+_R\right)}{\Lambda^2_{\chi_0}} \quad (29)$$

$$\mathcal{O}^{nlo}_{2+} = \frac{\text{Tr}\left(\partial_\mu\Sigma^\dagger\tau^+_{LR}\partial^\mu\Sigma^\dagger\tau^+_{LR} + \partial_\mu\Sigma\tau^+_{RL}\partial^\mu\Sigma\tau^+_{RL}\right)}{2\Lambda^2_{\chi_0}} \quad (30)$$

$$\mathcal{O}^{nlo}_{3+} = \frac{\text{Tr}\left(\Sigma\chi^\dagger_+\tau^+_L\Sigma\chi^\dagger_+\tau^+_L + \Sigma^\dagger\chi_+\tau^+_R\Sigma^\dagger\chi_+\tau^+_R\right)}{\Lambda^4_{\chi_0}} \quad (31)$$

where $\chi_+ = 2Bm_Q$ and with the same overall prefactor as in Eq. (22).

The hadronic contribution to the various transition amplitudes (factor off the $\bar{e}e^c\frac{G_F^2}{\Lambda_{\beta\beta}}c^W_i$ prefactor) are given through NLO in the chiral expansion

$$O_1 = \frac{\beta_1\Lambda^4_{\chi_0}}{(4\pi)^2}\left[1 - \frac{5}{3}\epsilon^2_\pi\ln(\epsilon^2_\pi) + c_1\epsilon^2_\pi\right] \,, \quad (32)$$

$$O_2 = \frac{\beta_2\Lambda^4_{\chi_0}}{(4\pi)^2}\left[1 - \frac{5}{3}\epsilon^2_\pi\ln(\epsilon^2_\pi) + c_2\epsilon^2_\pi\right] \,, \quad (33)$$

$$\frac{O_3}{\epsilon^2_\pi} = \frac{\beta_3\Lambda^4_{\chi_0}}{(4\pi)^2}\left[1 - \frac{8}{3}\epsilon^2_\pi\ln(\epsilon^2_\pi) + c_3\epsilon^2_\pi\right] \,, \quad (34)$$

where

$$\epsilon_\pi = \frac{m_\pi}{4\pi F_\pi} \,, \quad (35)$$

the LECs of the NLO counterterms are given by $\beta_i c_i$ and the dim-reg scale has been set to $\mu = 4\pi F_\pi$. The chiral extrapolation functions for the color-mixed operators are identical in form to their color-unmixed counterparts.

These expressions are determined with dimensional-regularization with the modified minimal subtraction scheme common for χPT calculations [57]. When performing chiral extrapolations, the use of on-shell renormalized quantities tends to improve the behavior of the perturbative χPT extrapolation [104, 112, 113]. We find this to be true in the present work as well, using an extrapolation with $\Lambda_{\chi_0} \to \Lambda_\chi = 4\pi F_\pi(m_\pi)$, in which case the extrapolation formulas are given in Eq. (7),

$$O_1 = \frac{\beta_1\Lambda^4_\chi}{(4\pi)^2}\left[1 + \frac{7}{3}\epsilon^2_\pi\ln(\epsilon^2_\pi) + \tilde{c}_1\epsilon^2_\pi\right] \,,$$

$$O_2 = \frac{\beta_2\Lambda^4_\chi}{(4\pi)^2}\left[1 + \frac{7}{3}\epsilon^2_\pi\ln(\epsilon^2_\pi) + \tilde{c}_2\epsilon^2_\pi\right] \,,$$

$$\frac{O_3}{\epsilon^2_\pi} = \frac{\beta_3\Lambda^4_\chi}{(4\pi)^2}\left[1 + \frac{4}{3}\epsilon^2_\pi\ln(\epsilon^2_\pi) + \tilde{c}_3\epsilon^2_\pi\right] \,,$$

where $\tilde{c}_i = c_i - 4(4\pi)^2 l^r_4(\Lambda_\chi)$, with $l^r_4(\mu)$ being the Gasser-Leutwyler coefficient which renormalizes F_π at NLO.

In order to generalize the extrapolation function to our finite-volume mixed-action lattice action, we begin with the partially quenched derivation. For $SU(4|2)$ the 2×2 ϕ field is extended to a 6×6 matrix with indices running over the valence, sea and ghost sectors of the theory. The Tr turn into sTr corresponding to the graded algebra. The derivation of the partially quenched expression is straight forward and gives rise to dependence upon both the valence-valence pions, which we denote π, and the mixed valence-sea pions we denote with a vs. The $\langle\pi|\mathcal{O}^{++}_{2+}|\pi\rangle$ matrix element receives a contribution from the hairpin contributions [109, 110].

To account for the finite volume corrections, we simply replace the tadpole integral by its finite volume counterpart

$$\mathcal{I}(m, mL) = \int \frac{d^4k}{(4\pi)^4}\frac{i}{k^2 - m^2 + i\epsilon} + \frac{4m^2}{(4\pi)^2}\sum_{|\mathbf{n}|\neq \mathbf{0}}\frac{K_1(mL|\mathbf{n}|)}{mL|\mathbf{n}|} \,. \quad (36)$$

Using the χPT standard dimensional regularization with a modified minimal subtraction, the infinite volume tadpole integral takes its standard form

$$\mathcal{I}(m) = \frac{m^2}{(4\pi)^2}\ln\left(\frac{m^2}{\mu^2}\right) \,. \quad (37)$$

The partially-quenched hairpin contribution can be isolated to a contribution with an integral [103]

$$\mathcal{I}^{PQ}(m) = \int \frac{d^4k}{(4\pi)^4}\frac{i\Delta^2_{PQ}}{(k^2 - m^2 + i\epsilon)^2} \,, \quad (38)$$

TABLE III. These LECs and the corresponding correlation matrix, determined from the MAEFT analysis, are provided with our Jupyter notebook [66]. Users can also try different extrapolation ansatz prescribed in the notebook.

β_1	c_1	β_1'	c_1'	β_2	c_2	β_2'	c_2'	β_3	c_3
-1.88(12)	4.0(1.3)	-6.99(45)	3.8(1.3)	-3.56(26)	2.4(1.3)	1.063(80)	1.2(1.2)	1.093(63)	9.0(2.0)

where $\Delta_{PQ}^2 \equiv m_{\pi,sea}^2 - m_{\pi,val}^2$. This integral can be determined from the relation

$$\mathcal{I}^{PQ}(m) = \Delta_{PQ}^2 \frac{\partial}{\partial m^2} \mathcal{I}(m)\,, \tag{39}$$

which can also be used to determine the enhanced finite volume correction from this hairpin contribution,

$$\mathcal{I}(m, mL) = \frac{1 + \ln(m^2/\mu^2)}{(4\pi)^2} - 2 \sum_{|\mathbf{n}|\neq \mathbf{0}} \frac{K_0(mL|\mathbf{n}|)}{(4\pi)^2}\,. \tag{40}$$

Finally, at NLO in the MAEFT, the MA extrapolation formula can be determined directly from the corresponding PQ formula with the addition of counterterm contributions arising from the discretization [105].

$$\begin{aligned} O_1 = \frac{\beta_1 \Lambda_\chi^4}{(4\pi)^2} \Bigg[& 1 + 2\epsilon_{vs}^2 \ln(\epsilon_{vs}^2) + \frac{1}{3}\epsilon_\pi^2 \ln(\epsilon_\pi^2) + c_1' \epsilon_\pi^2 + \alpha_1 \epsilon_a^2 - 8\epsilon_{vs}^2 f_1(m_{vs}L) + \frac{4}{3}\epsilon_\pi^2 f_1(m_\pi L) \\ & + \alpha_1^{(4)} \epsilon_a^4 + c_1^{(4)} \epsilon_\pi^4 + m_1 \epsilon_a^2 \epsilon_\pi^2 \Bigg]\,, \end{aligned} \tag{41}$$

$$\begin{aligned} O_2 = \frac{\beta_2 \Lambda_\chi^4}{(4\pi)^2} \Bigg[& 1 + 2\epsilon_{vs}^2 \ln(\epsilon_{vs}^2) + \frac{1}{3}\epsilon_\pi^2 \ln(\epsilon_\pi^2) + c_2' \epsilon_\pi^2 + \alpha_2 \epsilon_a^2 - 8\epsilon_{vs}^2 f_1(m_{vs}L) + \frac{4}{3}\epsilon_\pi^2 f_1(m_\pi L) \\ & - 2\epsilon_{PQ}^2 \left[1 + \ln(\epsilon_\pi^2) - 2 f_0(m_\pi L)\right] + \alpha_2^{(4)} \epsilon_a^4 + c_2^{(4)} \epsilon_\pi^4 + m_2 \epsilon_a^2 \epsilon_\pi^2 \Bigg]\,, \end{aligned} \tag{42}$$

$$\begin{aligned} \frac{O_3}{\epsilon_\pi^2} = \frac{\beta_3 \Lambda_\chi^4}{(4\pi)^2} \Bigg[& 1 + 2\epsilon_{vs}^2 \ln(\epsilon_{vs}^2) - \frac{2}{3}\epsilon_\pi^2 \ln(\epsilon_\pi^2) + c_3' \epsilon_\pi^2 + \alpha_3 \epsilon_a^2 - 8\epsilon_{vs}^2 f_1(m_{vs}L) - \frac{8}{3}\epsilon_\pi^2 f_1(m_\pi L) \\ & + \alpha_3^{(4)} \epsilon_a^4 + c_3^{(4)} \epsilon_\pi^4 + m_3 \epsilon_a^2 \epsilon_\pi^2 \Bigg]\,, \end{aligned} \tag{43}$$

where we have defined

$$f_0(mL) = \sum_{|\mathbf{n}|\neq \mathbf{0}} K_0(mL|\mathbf{n}|)\,, \tag{44}$$

$$f_1(mL) = \sum_{|\mathbf{n}|\neq \mathbf{0}} \frac{K_1(mL|\mathbf{n}|)}{mL|\mathbf{n}|}\,. \tag{45}$$

The small expansion parameters are defined for our mixed action [36]

$$\epsilon_\pi \equiv \frac{m_\pi}{4\pi F_\pi}\,, \qquad \epsilon_{vs} \equiv \frac{m_{vs}}{4\pi F_\pi}\,,$$
$$\epsilon_{PQ}^2 \equiv \frac{a^2 \Delta_I}{(4\pi F_\pi)^2}\,, \qquad \epsilon_a^2 \equiv \frac{1}{4\pi}\frac{a^2}{w_0^2}\,, \tag{46}$$

where $w_0 \sim 0.17$ fm is a gradient-flow scale [114]. With the tuning of the valence quark masses we have chosen [36], in the limit $a \to 0$, $m_{vs} \to m_\pi$, and these expressions go to those in Eq. (7) as $m_\pi L \to \infty$. We have added counter terms from next-to-next-to-leading order in the chiral expansion to estimate the uncertainty arising from truncating the chiral and continuum limit extrapolations. The resulting LECs from this analysis are provided in Tab. III. The full extrapolation analysis is provided in our Jupyter notebook [66], which also allows users to explore different extrapolation functions.

Similar analyses were performed to determine the pion bag parameter, B_π, as discussed in the main text. In Fig. 4, we display the pion mass dependence of B_π.

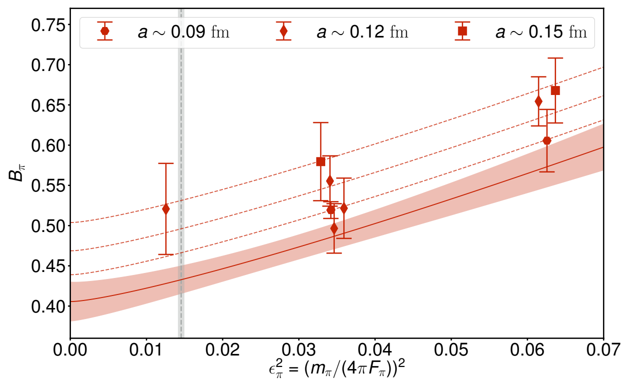

FIG. 4. The interpolation of $B_\pi = O_3/(\frac{8}{3}m_\pi^2 F_\pi^2)$. The (red) band represent the 68% confidence interval of the continuum, infinite volume extrapolated value of the matrix elements. The vertical gray band highlights the physical pion mass.